Spectroscopy and Dynamics of a Two-Dimensional Electron Gas on Ultrathin Helium Films on Cu(111)

N. Armbrust, J. Güdde, and U. Höfer

Fachbereich Physik und Zentrum für Materialwissenschaften, Philipps-Universität, 35032 Marburg, Germany

S. Kossler and P. Feulner

Physikdepartment E20, Technische Universität München, 85747 Garching, Germany

Electrons in image-potential states on the surface of bulk helium represent a unique model system of a two-dimensional electron gas. Here, we investigate their properties in the extreme case of reduced film thickness: a monolayer of helium physisorbed on a single-crystalline (111)-oriented Cu surface. For this purpose we have utilized a customized setup for time-resolved two-photon photoemission at very low temperatures under ultrahigh vacuum conditions. We demonstrate that the highly polarizable metal substrate increases the binding energy of the first ($n = 1$) image-potential state by more than 2 orders of magnitude as compared to the surface of liquid helium. An electron in this state is still strongly decoupled from the metal surface due to the large negative electron affinity of helium and we find that even 1 monolayer of helium increases its lifetime by 1 order of magnitude compared to the bare Cu(111) surface.

Two-dimensional (2D) electron systems have attracted interest for more than 40 years. Apart from sheet structures such as graphene, 2D electron systems exist at heterostructures like semiconductor-semiconductor [1,2], semiconductor-insulator [2–4], oxide-oxide [5], or metal-insulator interfaces [6], and on the surface of condensed materials with a negative electron affinity [4,7,8]. Two limiting cases are known: dense electron layers with Fermi temperatures in the hundred K range in quantum wells, particularly of semiconductor heterostructures [1,2]; and very dilute 2D electron gases in the image-potential states on top of condensed helium [4,7,8] with Fermi temperatures in the mK range, and spacing of the excited states in the microwave regime [9]. For electrons on the bulk surface of He, the maximum density is small: for more than $\approx 2 \times 10^9$ electrons per cm^{-2} the layer becomes unstable [10] and the electron gas remains in the classical regime. Early, it was realized that the density of such electron layers can be significantly increased by growing He films of finite thickness on top of a substrate with large permittivity [11,12]. For a 100 Å He film on a doped silicon substrate, for example, densities of up to 10^{11} cm^{-2} have been reported [13]. Such densities offer the possibility to study the quantum regime of this almost ideal 2D electron system including effects such as Wigner crystallization and quantum-melting [12] as long as the electron gas is well decoupled from the substrate. For very thin films, however, the coupling to the substrate will be strongly influenced by surface roughness and impurities of the substrate that can lead to lateral localization and enhanced tunneling through the film [13,14]. The study of this regime thus requires the combination of advanced surface science and cryogenic techniques.

In this Letter, we investigate the limiting case of a monolayer (ML) of He on an atomically flat single-crystalline metal substrate and present a study of the electron transfer dynamics of the image-potential states on this archetypical 2D system. Image potential states on clean and rare gas covered metal surfaces already proved to be ideal model systems for the electron transfer dynamics at surfaces and through thin dielectric layers, by theory and by experiment, in particular, by two-photon photoemission (2PPE) studies [15]. For thin films of the heavier rare gases, it has been shown that the coupling of the image-potential states to the metal strongly depends on the electron affinity of the film, which represents a tunnel barrier in the case of negative electron affinity [6,16–18]. He films are expected to exhibit a particularly high barrier (the electron affinity of condensed He is −1.3 eV [19]), which offers the possibility to create a 2D electron gas with high binding energy and very long lifetime, even for very small thicknesses. He films are also unique with regard to their structure. Whereas all other rare gases, including Neon, form islands at submonolayer coverage and solid single crystals at larger thicknesses [18,20–22], the submonolayer of He grows as a uniform 2D gas layer, and thick He films are liquid because of the large zero-point energy and the weak van der Waals interaction [23]. Despite these outstanding quantum properties, the 2D electron gas on ultrathin He films was not investigated until now, mainly because of experimental challenges.

2PPE of He films requires very low temperatures [24,25], shielding from thermal radiation of the environment, which leads to desorption of the layers [24,25], and highly sensitive electron spectroscopy at low laser
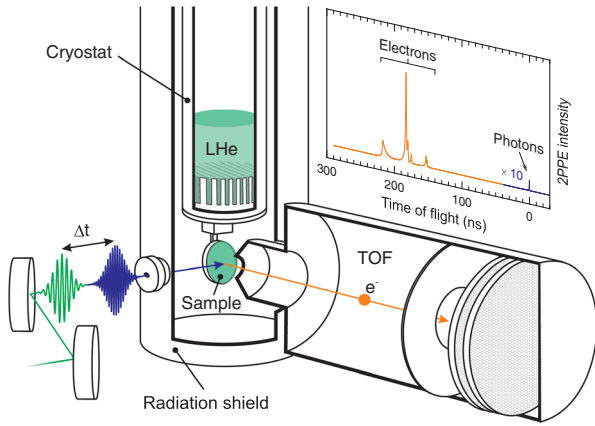
FIG. 1.   Cut-away view onto the cryostat, the sample mount, the TOF spectrometer, and the light path. The 80 K radiation shields surrounding the cryostat, sample mount, and spectrometer were brought in seamless contact upon He layer preparation and data acquisition. The laser beams were focused onto the sample through a 2 mm^2 aperture in the radiation shield at an 80° angle of incidence. The inset shows a typical TOF spectrum with the consecutive arrival of scattered uv photons and photoelectrons.

intensities. Tackling these challenges with customized equipment, we present results on binding energies and lifetimes of the image potential states on ultrathin He films physisorbed on a single-crystalline Cu(111) substrate.

Figure 1 shows the experimental setup. The liquid He (LHe) bath cryostat of our UHV chamber (base pressure of 5×10^{-11} mbar) was operated at a He pressure of typically 5×10^{-2} mbar corresponding to a LHe temperature below 1 K [26]. Well-defined Cu(111) surfaces have been prepared by *in situ* epitaxial growth of approximatly 100 ML thick Cu films on a Ru(0001) single crystal. The latter was thermally coupled to the cryostat by a thin, spot-welded single-crystalline tungsten rod. With this setup, sample temperatures below 1.2 K were obtained [27,28]. He films were prepared by dosing purified He gas through a capillary aiming at the sample. We compensated for the unavoidable loss of He due to laser stimulated desorption by a controlled continuous flow of He, which allows for the variation of the adlayer density within the laser spot. Further details of the sample preparation and characterization are described in the Supplemental Material [29].

In order to avoid electronically stimulated desorption of the He layers by the 300 K blackbody radiation of the environment [24,25], the whole cryostat and the time-of-flight (TOF) spectrometer used for electron spectroscopy (≤ 20 meV energy resolution) were surrounded by radiation shields cooled to 80 K by liquid nitrogen (LN$_2$) [27,28]. During the experiment, these shields were completely closed except of a tiny 2 mm^2 aperture for the laser beams (Fig. 1).
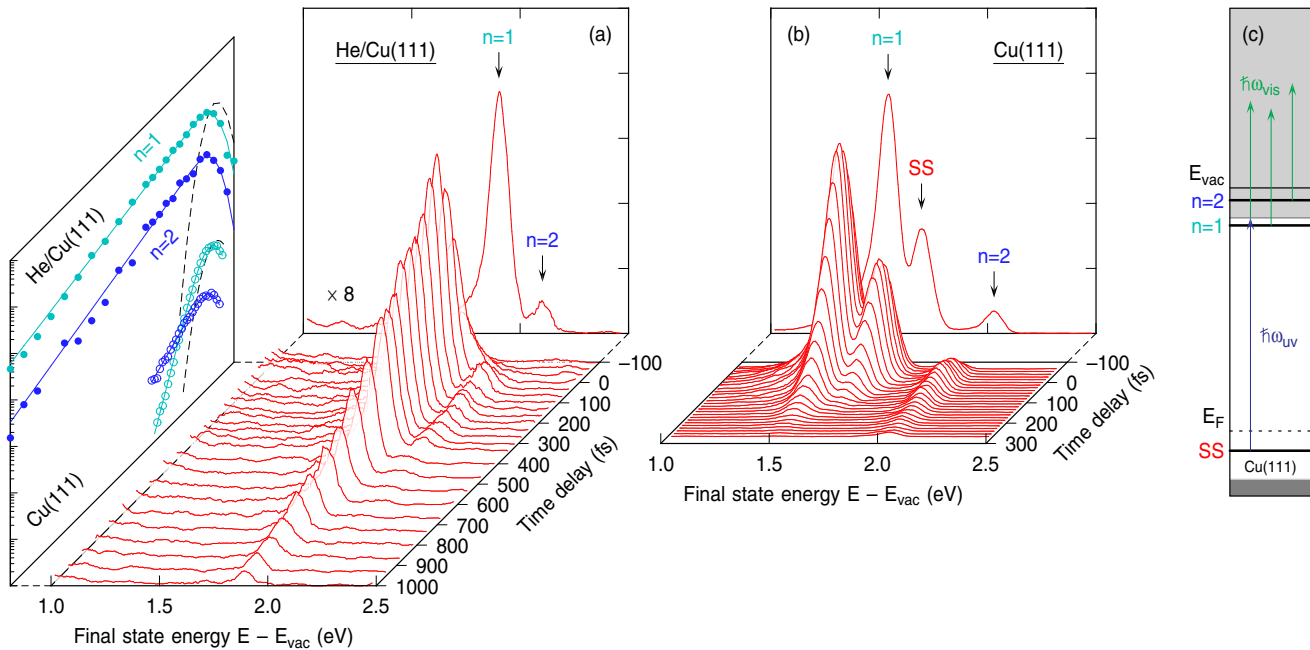

FIG. 2.   2PPE spectra from (a) a saturated He monolayer and (b) the pristine Cu(111) surface for different time delays Δt between pump and probe pulses, according to the excitation scheme in (c). The rear panels in (a) and (b) show 2PPE spectra for $\Delta t \approx 0$ with maxima assigned to the image-potential states ($n = 1, 2$) and the Shockley-type surface state (SS). The left panel with logarithmic intensity scale shows transient 2PPE data of the ($n = 1, 2$) states (cyan and blue symbols) for pristine Cu(111) (circles) and for He monolayer (dots). The solid lines in this panel show best fits of a rate-equation model assuming single-exponential decay. The dashed lines indicate the cross-correlation of the pump and probe pulses obtained from the signal of the nonresonantly emitted Shockley state for the pristine (bottom) and He-covered surface (top).

The laser setup provided p-polarized femtosecond laser pulses in the visible (vis) and ultraviolet (uv) spectral range with variable time delay Δt at a repetition rate of 250 kHz [31]. Typical photon energies and pulse lengths of $\hbar\omega_{\mathrm{vis}} = 2.28$ eV, $\tau_{\mathrm{vis}} = 50$ fs and $\hbar\omega_{\mathrm{uv}} = 4.56$ eV, $\tau_{\mathrm{uv}} = 80$ fs enabled excitation of the first two image-potential states with the uv pulses but simultaneously avoided an excessive background signal due to one-photon photoemission. The average laser power of each laser beam was reduced to only ~ 50 μW (~ 0.2 nJ/pulse) as a compromise between He desorption and 2PPE intensity.

Figure 2 shows two time-resolved series of 2PPE spectra at normal emission obtained from the He covered (a) and bare (b) Cu(111) surface. Both series show three prominent features. The peaks denoted as $n = 1$ and $n = 2$ are assigned to the first two members of the Rydberg-like series of initially unoccupied image-potential states that are populated by the uv pump pulses and subsequently photo-emitted by the vis probe pulses, as illustrated in (c) [38]. The signals of the ($n = 1$) and ($n = 2$) states appear for the bare surface at final state energies of 1.55 and 2.05 eV, respectively [rear panel of (b)]. This corresponds to binding energies with respect to E_{vac} of $E_{n=1} = 0.73 \pm 0.03$ and $E_{n=2} = 0.24 \pm 0.03$ eV. We note that theses binding energies are slightly smaller than values reported for Cu(111) bulk samples [21,30–32]. The peak at 1.71 eV denoted by SS results from direct photoemission from the partially occupied intrinsic Shockley-type surface state by nonresonant 2PPE with one uv and one vis photon and is only visible for temporal overlapping pump and probe pulses. At the $\bar{\Gamma}$ point this state has a binding energy of $E_{\mathrm{SS}} = 0.39 \pm 0.05$ eV with respect to the Fermi level.

The 2PPE spectra of the He covered Cu(111) surface of Fig. 2(a) have been recorded at a He background pressure p_{He} of 5×10^{-8} mbar, which supports a coverage of 1 ML under laser irradiation, as will be shown. Compared to the pristine Cu(111) surface the signal of the SS is almost completely quenched and the ($n = 1$) and ($n = 2$) maxima show a considerable blueshift to final states energies of 1.94 and 2.13 eV with respect to E_{vac}, respectively. At these energies, also the ($n = 1$) state is degenerated with the projected Cu bulk bands [Fig. 3] and is, in fact, an image-potential resonance.

The energy shift is almost completely caused by a reduction of the binding energies by about a factor of two ($E_{n=1} = 0.35 \pm 0.03$ eV, $E_{n=2} = 0.16 \pm 0.03$ eV), whereas the weakly polarizable He film reduces the work function Φ only marginally by 50 meV [Fig. 3]. Thus, even one monolayer of He strongly decouples the image-potential states from the metal surface. Despite this decoupling, the binding energies are much larger than those reported for electrons on the surface of LHe ($E_{n=1} \sim 1$ meV [39]), because of the strong electron attraction by the highly polarizable metal substrate underneath the He film.
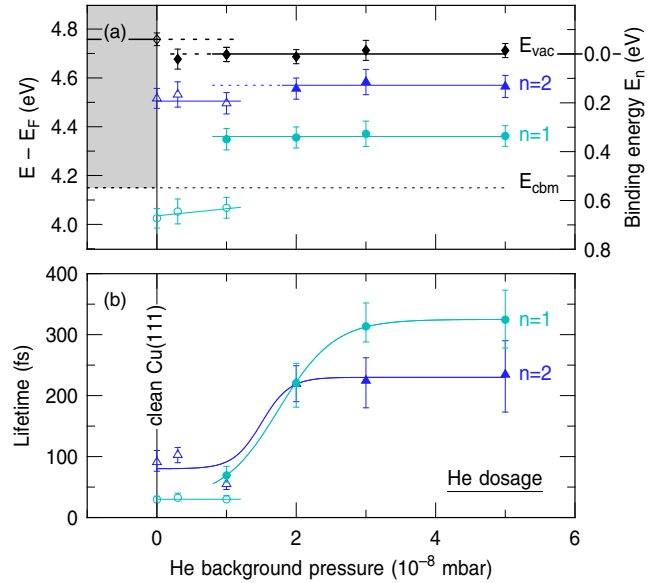

FIG. 3. (a) Energy with respect to the Fermi level E_F and (b) lifetimes of the image-potential states $n = 1$ and $n = 2$ as a function of the He background pressure (green and blue data points, the solid lines are a guide for the eye). Open (solid) symbols depict data assigned to the bare (He covered) surface. Black data points represent the position of the vacuum level which serves as reference for the binding energy E_n. The shaded gray area depicts the projected bulk bands at the $\bar{\Gamma}$ point of Cu(111).

Lifetimes of electrons excited into the image-potential states at the $\bar{\Gamma}$ point have been determined by measuring the 2PPE intensity at the respective energies as function of the time delay between the uv and the vis laser pulses [Fig. 2, left panel]. The lifetimes have been extracted from best fits (solid lines) using a rate-equation model assuming single-exponential population decay. On the bare Cu(111) surface, the states $n = 1$ and $n = 2$ show lifetimes of $\tau_{n=1} = 34 \pm 5$ and $\tau_{n=2} = 108 \pm 15$ fs, respectively [29].

Adsorption of a monolayer of He drastically changes the electron dynamics in the image-potential states: $\tau_{n=1}$ increases by 1 order of magnitude to 330 ± 60 fs [Fig. 3(b)], despite the fact that the $n = 1$ state becomes an image-potential resonance. The lifetime of the ($n = 2$) state, which is already an image-potential resonance on the bare Cu(111) surface, is less affected. It increases only by a factor of 2 to 256 ± 60 fs.

For coverage dependent data, the He density within the illuminated spot has been calibrated by systematic 2PPE measurements as a function of p_{He}, while keeping the laser intensities constant. The results are summarized in Fig. 3 where $E_{n=1,2}$ (a) and $\tau_{n=1,2}$ (b) are plotted as a function of p_{He}. For increasing p_{He}, Φ slightly drops by only 50 meV. The peaks assigned to the ($n = 1, 2$) states on the pristine Cu surface decrease continuously and vanish for $p_{\mathrm{He}} > 1 \times 10^{-8}$ mbar. Simultaneously, two new peaks with lower binding energies appear in the 2PPE spectrum,

which we assign to the first two image-potential states on the He covered areas. Just at $p_{He} = 1 \times 10^{-8}$ mbar, we still observe the ($n = 1$) peak assigned to the uncovered areas and already the ($n = 1$) peak assigned to the covered areas [29]. This might be surprising at first glance, since submonolayers of physisorbed He do not grow as 2D islands like the heavier rare gases, but form instead a 2D gas. In our experiment, the coexistence of covered and uncovered areas results from the competition of adsorption and laser induced desorption, which causes a variation of the coverage across the spot profile of the laser. The desorption rate is, however, small. We estimate it to be $< 10^{-7}$ ML per laser shot [29]. The assignment of the states is consistent with their lifetimes as a function of p_{He}. The lifetimes of the states assigned to bare Cu(111) areas remain almost constant while those of the states assigned to the He covered areas increase with p_{He} and saturate above $p_{He} = 2 \times 10^{-8}$ mbar, which we interpret as the formation of a saturated monolayer. We do not expect the formation of the more weakly bound second monolayer [29].

On the Cu(111) surface, the change of the decay dynamics upon He adsorption is an interplay of decoupling of the wave functions from the metal and energy shift with respect to the Cu bulk bands. Whereas the decoupling increases the lifetime, the shift into resonance with the Cu bulk bands reduces it, because it opens the additional decay channel of elastic resonant charge transfer into the bulk [32,34].

The decoupling is caused by the strong Pauli repulsion by the closed-shell He atoms. This repulsion constitutes a high tunneling barrier for the whole series of image-potential states and extends up to 1.3 eV above the vacuum level for a thick layer of liquid He [19]. The image force attraction induced by the metal substrate reduces this barrier, whereas the larger density of the monolayer due to the much stronger He-metal compared to He-He dispersion forces increases it [40]. The actual barrier height can be estimated from the above-threshold maximum of the kinetic energy distributions of secondary electrons, which in good approximation corresponds to the top of the barrier with respect to the vacuum level. Our data and those of Ref. [27] yield 0.8 eV for this quantity; in combination with the ($n = 1, 2$) binding energies this results in effective barrier heights of 1.15 and 0.96 eV for the ($n = 1$) and ($n = 2$) states, respectively.

These barriers push the image-potential states further away from the metal and strongly reduce the wave function overlap with the Cu bulk and surface states. This overlap is the crucial quantity for the lifetime of image-potential states and resonances, because it determines the efficiency of both inelastic and elastic decay [15,32]. The latter dominates the decay of image-potential resonances and is responsible for their general much shorter lifetimes as compared to image-potential states at the same barrier height [31]. Against this background, the observed increase of the ($n = 1$) lifetime

on Cu(111) by 1 order of magnitude is unprecedentedly large and clearly opens up new possibilities for detailed investigations of 2D electron gases.

In the framework of the present study, the choice of Cu(111) films on Ru(0001) as a substrate was dictated by technical constraints. In a further optimized experimental setup one would make use of substrates like Cu(100) or Ag(100), on which the image-potential states are located far from the projected bulk bands [41]. The present data allow us to predict the degree of decoupling by a He layer on these substrates by comparing the measured ($n = 1$)-resonance lifetime of He/Cu(111) with that of a hypothetical resonance on bare Cu(111) at the same energy. The dominant elastic contribution of its lifetime can be calculated reliably within a multiple scattering approach that provides the electron reflectivity r_C at the surface barrier as a function of energy [34]. Potential parameters of Cu(111) [41] yield for this quantity 0.74 (0.65) at an energy of 0.1 eV (0.2 eV) above the band edge, which corresponds to an elastic lifetime of only 4 fs (2.9 fs). Even if we allow an uncertainty of the exact band edge position in our Cu(111) films of 0.1 eV, this estimation demonstrates that the decoupling of a single ML of He is capable of enhancing the ($n = 1$) lifetime by up to 2 orders of magnitude. This is about 30 times larger as compared to Ar [16].

In conclusion, we have shown that the ultimate model system of a 2D electron gas on a thin He film grown on an atomically smooth single crystalline metal surface is accessible with time-resolved photoemission spectroscopy. We find that its lifetime is under such conditions only limited by tunneling and not by surface defects. In a further optimized setup, which reaches temperatures below 1 K as required for the growth of thicker He layers, our results let us expect to realize lifetimes of several hundred picoseconds even on an only 2-ML-thick He film on Cu(100) or Ag(100). The binding energy on such a thin film is still large enough to support high electron densities without becoming instable due to ripplon formation [13]. In combination with angle-resolved photoemission spectroscopy, this opens the possibility to observe phenomena such as Wigner crystallization and melting into a degenerate 2D electron gas within momentum space.

[1] H. L. Störmer, R. Dingle, A. C. Gossard, W. Wiegmann, and M. D. Sturge, Solid State Commun. **29**, 705 (1979).
[2] J. Davies, *The Physics of Low-dimensional Semiconductors: An Introduction* (Cambridge University Press, Cambridge, England, 1998).

[3] T. Ando, A. B. Fowler, and F. Stern, Rev. Mod. Phys. **54**, 437 (1982).

[4] Y. P. Monarkha and K. Kono, *Two-Dimensional Coulomb Liquids and Solids* (Springer-Verlag, Berlin, Heidelberg, 2004).

[5] S. Stemmer and S. J. Allen, Annu. Rev. Mater. Res. **44**, 151 (2014).

[6] J. Güdde and U. Höfer, Prog. Surf. Sci. **80**, 49 (2005).

[7] M. W. Cole, Rev. Mod. Phys. **46**, 451 (1974).

[8] *Two-Dimensional Electron Systems*, edited by E. Y. Andrei (Kluwer Academic, Dordrecht, Netherlands, 1997).

[9] C. C. Grimes, T. R. Brown, M. L. Burns, and C. L. Zipfel, Phys. Rev. B **13**, 140 (1976).

[10] V. S. Edel'man, Sov. Phys. Usp. **23**, 227 (1980).

[11] H. Ikezi and P. M. Platzman, Phys. Rev. B **23**, 1145 (1981).

[12] F. M. Peeters and P. M. Platzman, Phys. Rev. Lett. **50**, 2021 (1983).

[13] H. Etz, W. Gombert, W. Idstein, and P. Leiderer, Phys. Rev. Lett. **53**, 2567 (1984).

[14] T. Günzler, B. Bitnar, G. Mistura, S. Neser, and P. Leiderer, Surf. Sci. **361–362**, 831 (1996).

[15] P. M. Echenique, R. Berndt, E. V. Chulkov, T. Fauster, A. Goldmann, and U. Höfer, Surf. Sci. Rep. **52**, 219 (2004).

[16] W. Berthold, P. Feulner, and U. Höfer, Chem. Phys. Lett. **358**, 502 (2002).

[17] D. C. Marinica, C. Ramseyer, A. G. Borisov, D. Teillet-Billy, J. P. Gauyacq, W. Berthold, P. Feulner, and U. Höfer, Phys. Rev. Lett. **89**, 046802 (2002).

[18] W. Berthold, F. Rebentrost, P. Feulner, and U. Höfer, Appl. Phys. A **78**, 131 (2004).

[19] W. T. Sommer, Phys. Rev. Lett. **12**, 271 (1964).

[20] H. Schlichting and D. Menzel, Surf. Sci. **272**, 27 (1992).

[21] M. Wolf, E. Knoesel, and T. Hertel, Phys. Rev. B **54**, R5295 (1996).

[22] W. Berthold, P. Feulner, and U. Höfer, Surf. Sci. **548**, L13 (2004).

[23] A phase transition, which might be interpreted as solidification, has been observed for He/Pt(111) at coverages beyond 70% of saturation by means of thermal desorption spectroscopy [24,25]. This transition, however, could not be verified by electron spectroscopy as yet [27,28].

[24] T. Niedermayer, H. Schlichting, D. Menzel, S. H. Payne, and H. J. Kreuzer, Phys. Rev. Lett. **89**, 126101 (2002).

[25] T. Niedermayer, H. Schlichting, D. Menzel, S. H. Payne, and H. J. Kreuzer, Phys. Rev. B **71**, 045427 (2005).

[26] J. R. Clement, J. K. Logan, and J. Gaffney, Phys. Rev. **100**, 743 (1955).

[27] S. Kossler, Dissertation, Technische Universität München, 2011, http://nbn-resolving.de/urn/resolver.pl?urn:nbn:de:bvb:91-diss-20110927-1079140-1-2.

[28] S. Kossler, P. Feulner, and J.-P. Gauyacq, Phys. Rev. B **89**, 165410 (2014).

[29] See Supplemental Material at http://link.aps.org/supplemental/10.1103/PhysRevLett.116.256801 for further information about sample preparation and characterization, formation of a second He layer, laser induced desorption, and additional spectra at different He background pressures, which includes Refs. [18,21,25,27,28,30–37].

[30] M. Weinelt, J. Phys. Condens. Matter **14**, R1099 (2002).

[31] A. Damm, K. Schubert, J. Güdde, and U. Höfer, Phys. Rev. B **80**, 205425 (2009).

[32] A. G. Borisov, E. V. Chulkov, and P. M. Echenique, Phys. Rev. B **73**, 073402 (2006).

[33] K. Schubert, A. Damm, S. V. Eremeev, M. Marks, M. Shibuta, W. Berthold, J. Güdde, A. G. Borisov, S. S. Tsirkin, E. V. Chulkov, and U. Höfer, Phys. Rev. B **85**, 205431 (2012).

[34] U. Höfer and P. M. Echenique, Surf. Sci. **643**, 203 (2016).

[35] K. Tang and J. P. Toennies, Surf. Sci. **279**, L203 (1992).

[36] E. Zaremba and W. Kohn, Phys. Rev. B **15**, 1769 (1977).

[37] J. Perreau and J. Lapujoulade, Surf. Sci. **122**, 341 (1982).

[38] The ($n = 2$) state is, in fact, an image-potential resonance on Cu(111), because it is degenerated with Cu bulk bands [21,30–32].

[39] E. M. Cole and H. M. Cohen, Phys. Rev. Lett. **23**, 1238 (1969).

[40] J. R. Broomall, W. D. Johnson, and D. G. Onn, Phys. Rev. B **14**, 2819 (1976).

[41] E. V. Chulkov, V. M. Silkin, and P. M. Echenique, Surf. Sci. **437**, 330 (1999).